PAH Sorption Mechanism and Partitioning Behavior in Lampblack-Impacted Soils from Former Oil-Gas Plant Sites

LEI HONG,[†] UPAL GHOSH,[‡] TANIA MAHAJAN,[§,||] RICHARD N. ZARE,[§] AND RICHARD G. LUTHY*,[†]

Department of Civil and Environmental Engineering, Stanford University, Stanford, California 94305-4020, Department of Civil and Environmental Engineering, University of Maryland Baltimore County, Baltimore, Maryland 21250, and Department of Chemistry, Stanford University, Stanford, California 94305-5080

This study assessed polycyclic aromatic hydrocarbon (PAH) association and aqueous partitioning in lampblack-impacted field soils from five sites in California that formerly housed oil−gas process operations. Lampblack is the solid residue resulting from the decomposition of crude oil at high temperatures in the gas-making operation and is coated or impregnated with oil gasification byproducts, among which PAHs are the compounds of the greatest regulatory concern. A suite of complementary measurements investigated the character of lampblack particles and PAH location and the associated effects on PAH partitioning between lampblack and water. PAH analyses on both whole samples and density-separated components demonstrated that 81−100% of PAHs in the lampblack-impacted soils was associated with lampblack particles. FTIR, ^{13}C NMR, and SEM analyses showed that oil−gas lampblack solids comprise primarily aromatic carbon with soot-like structures. A free-phase aromatic oil may be present in some of the lampblack soils containing high PAH concentrations. Comparable long-term aqueous partitioning measurements were obtained with an air-bridge technique and with a centrifugation/alum flocculation procedure. Large solid/water partition coefficient (K_d) values were observed in samples exhibiting lower PAH and oil levels, whereas smaller K_d values were measured in lampblack samples containing high PAH levels. The former result is in agreement with an oil−soot partitioning model, and the latter is in agreement with a coal tar−water partitioning model. Lampblack containing high PAH levels appears to exhaust the sorption capacity of the soot−carbon, creating a free aromatic oil phase that exhibits partitioning behavior similar to PAHs in coal tar. This study improves mechanistic understanding of PAH sorption on aged lampblack residuals at former oil−gas sites and provides a framework for mechanistic assessment of PAH leaching potential and risk from such site materials.

* Corresponding author e-mail: luthy@Stanford.edu; phone: (650)725-9170; fax: (650)725-3164.

[†] Department of Civil and Environmental Engineering, Stanford University.

[‡] Department of Civil and Environmental Engineering, University of Maryland Baltimore County.

[§] Department of Chemistry, Stanford University.

[||] Present address: Celera, South San Francisco, CA.

Introduction

Prior to the widespread distribution of natural gas, manufactured gas from coke, coal, and oil served as the major gaseous fuel for urban heating, cooking, and lighting in the US for over 100 years. In the eastern United States, where coal was plentiful, gas was derived from coal or coke. Along the West Coast, because of the availability of oil and the expense in transporting coal or coke to this region, gas was made by gasifying oil in refractory-lined generators. The first large-scale oil−gas process in the West was installed in Oakland, CA, in 1902, and the so-called Pacific Coast oil−gas process was employed in numerous cities along the West Coast (*1*). The oil−gas process used a chamber of hot bricks, alternating between heating checker brick with air and oil and then making gas by atomizing oil with high-pressure steam. The process was based on the gasification and cracking of oil, wherein steam reacted with oil to yield CO, H_2, and CO_2 along with lampblack from the cracking of oil at high temperatures.

Lampblack Production. Lampblack and tar were byproducts of the oil−gas manufacturing process (*2*). The amount of lampblack formed varied with the type of process from 12 to 24 lb/1000 ft^3 of gas manufactured; about 3 lb of tar was produced per 1000 ft^3 of gas manufactured (*1*). Because of the small amount of tar made in the oil−gas manufacturing process, it was customary that lampblack was mixed with tar and used as boiler fuel or briquetted with a small amount of tar and sold as solid fuel. The pitch in the tar served to consolidate the particles of lampblack. In the 1920s, lampblack was a profitable byproduct when briquetted (*1*). The choice of process and amount of lampblack production depended on whether it was more economical to make lampblack or gas from the oil.

The recovery and disposal of the lampblack presented the biggest problems in the oil−gas manufacturing process (*1*). Lampblack collected on the surface of the washbox was amorphous as compared to gummy mixtures of tar and lampblack recovered from the bottom of the wash box (*1*). Modifications to the oil−gas process included separation of lampblack by filtering and forming gas by heating and blasting the lampblack with steam, which also distilled much of the volatile matter, and in this case tar was not deposited with the lampblack.

The production of lampblack on the West Coast could exceed demand, and lampblack was disposed by burning, briquetting, or dumping (*3*). Today, lampblack residues are commonly found at locations of former oil−gas processes. As outlined above, lampblack may contain various amounts of tar depending on process operations, method of recovery, briquetting operations, and disposal methods. The principal contaminants of concern are polycyclic aromatic hydrocarbons (PAHs). In comparison with coal tars from coal gasification and carbonization processes, comparatively little information is available on former oil−gas plant sites, on the properties of lampblack residues, and on how PAHs are distributed and associated among lampblack and geologic materials.

PAH Partitioning. PAHs sorb strongly to the organic carbon fraction of soil or sediment, with the solid organic carbon content typically used as a measure of sorption capacity (*4*). But because soils from oil−gas manufacturing

10.1021/es0262683 CCC: $25.00
Published on Web 00/00/0000

processes may contain solid lampblack (oil soot) and/or oil tar, these anthropogenic carbon forms in soil may exhibit sorption properties much different from natural soil organic matter. For example, in data compiled by Ghosh et al. (*5*), it is shown that the log partition coefficient (log K_{oc}) for phenanthrene sorbed on soot−carbon is 6.6 as compared to a log K_{oc} of 4−4.5 for natural organic carbons and an apparent log K_{oc} of 5.0 for coal tars. Thus, if PAHs are sorbed on soot-type carbon, the aqueous availability may be very much less as compared to PAHs associated with an oil phase or natural organic matter (*6*−*9*). Jonker and Koelmans (*10*) report PAH aqueous partitioning from several black carbon materials including oil soot. They observed that partition coefficients measured using added deuterated PAHs were much smaller than partition coefficients measured for the PAHs existing in the soot. They concluded that a fraction of PAHs present in the soot−carbon formed during soot formation are occluded in the microporous carbon matrix and are not available for aqueous partitioning. Thus, for soils impacted by oil−gas manufacturing process lampblack residues, a clear understanding of the nature of PAH sorption mechanisms is necessary to predict aqueous partitioning.

We investigated the properties of lampblack residues and the aqueous partitioning of PAHs in aged field materials by examination of lampblack samples from several former oil−gas plant sites in California. The project addressed the following questions.

(1) How are PAHs distributed among the soil mineral matter and lampblack in aged samples from former oil−gas manufacturing sites?

(2) How does the PAH fingerprint in lampblack residuals compare with weathered coal tar and commercial lampblack?

(3) How does the character of organic matter in oil−gas process lampblack residuals compare with that in soot, coal particles, natural organic matter, and commercial lampblack?

(4) How do PAHs partition between aged lampblack and water? Is the partitioning like that for soot or oil tar?

(5) What is an appropriate mechanistic perspective to describe the phase partitioning of PAHs between lampblack and water?

Materials and Methods

Lampblack residuals, intermixed with soils, were obtained from five different field sites in California that formerly housed oil−gas process operations. Lampblack residual samples are referred to as CA-2, CA-5, CA-10, CA-17, and CA-18, respectively, based on the location of the site from which they originated. The lampblack samples were obtained from site disposal locations and stored at 4 °C until used. For comparison, a commercial lampblack sample manufactured through an oil gasification process (Catalog No. C198-500) was obtained from Fisher Scientific (Pittsburgh, PA). Also for comparison, a weathered coal tar sample was obtained from a former manufactured gas plant site in Belvidere, IL, that employed a carbureted water gas process early in the 20th century. Extraction and analysis used pesticide-grade hexane, acetone, pentane, cyclohexane, and methylene chloride obtained from Fisher Scientific (Pittsburgh, PA). Soil total organic carbon (TOC) was determined by Scientific Environmental Lab, Inc. (Palo Alto, CA) using a combustion technique followed by nondispersive infrared (NDIR) detection (*11*).

PAH Analysis by Gas Chromatography-Flame Ionization Detection (GC-FID). PAH extraction from lampblack samples was performed by following EPA Method 3550B using 3 vol of 40 mL each of a hexane/acetone mixture (50:50) and sonicating the slurry for 6 min (pulsing for 15 s on and 15 s off). Following three sequential extractions, the extracts were combined, concentrated, and changed into solvent cyclohexane. Cleanup was performed on the final extract using a silica gel column as outlined in EPA Method 3630C. A gas chromatograph (Agilent model 6890) with a fused silica capillary column (HP-5, 30 m × 0.25 mm i.d.) and a flame ionization detector was used for analysis based on EPA Method 8100 for PAHs. A standard mixture of the 16 EPA priority pollutant PAHs obtained from Ultra Scientific Inc. (North Kingstown, RI) was used for calibration.

Density Separation and Surface Area Measurement. The field materials comprised lampblack intermixed with soil. Density separation removed the lampblack from the mineral matter (i.e., sand and clay). A saturated solution of cesium chloride with a specific gravity of 1.8 was used for density separation because the typical specific gravity of lampblack is about 1.77 (*12*) and is much smaller than that of sand/clay. Two grams of lampblack soil was mixed with 40 mL of cesium chloride solution and centrifuged at 2000 rpm for 10 min in a 50-mL glass centrifuge tube. The fine lampblack particles floated to the top and were decanted and collected on 0.7-μm glass fiber filter paper. This procedure was repeated 3−5 times until the lampblack fraction was separated from the heavier mineral fraction. The collected particles were washed with deionzied water to remove the residual cesium chloride. The mass of each fraction was recorded after air-drying and desiccating for 12 h. BET surface area was determined with nitrogen adsorption measurements at 77 K on a surface area and porosimetry system, COULTER SA 3100 (Coulter Corporation, Miami, FL), after degassing the sample at 373 K.

Microscale Analysis of PAHs. Microprobe two-step laser desorption/laser ionization mass spectrometry (μL^2MS) measurements of field samples were performed to characterize the distribution of PAHs present on the samples. Both whole samples and separated fractions of lampblack and sand/clay were analyzed. The use of the μL^2MS method for environmental organic geochemical work is described in Gillette et al. (*13*). The μL^2MS analysis involves desorption of PAH molecules from a particle or particles using a pulsed CO_2 laser (10.6 μm) focused to a circular spot with a diameter of 40 μm that would encompass a number of small particles. In the second step, the desorbed PAH molecules are selectively ionized with a pulsed UV laser (266 nm), and the resulting ions are extracted into a reflection time-of-flight mass spectrometer. The depth of penetration of the desorption laser is estimated to be between 0.5 and 1.0 μm based on test results with PAHs embedded in thin resin sections (*14*).

Scanning Electron Microscopy (SEM) and Elemental Analysis of Particles Surfaces. The micromorphology of extracted lampblack particles were examined by using a high-resolution Sirion SEM at ambient temperature and 5.0 kV. Samples were mounted on 12-mm carbon adhesive tabs and sputter-coated with Au−Pd alloy. Similar to the elemental analysis of dredged sediment particles with a SEM/WDX system as described by Ghosh et al. (*14*), measurement of the microscale elemental composition of lampblack particles was conducted using a Cameca SX-51 with a high-resolution quantitative energy dispersive spectrometer (EDS) system. The EDS system includes a beryllium as well as an atmospheric thin window for analysis of light elements, such as carbon and boron. Prior to EDS analysis, the particles were sputter-coated with silver.

Fourier Transform Infrared (FTIR) and Cross Polarization Magic Angle Spinning (CPMAS) ^{13}C Solid-State Nuclear Magnetic Resonance (NMR) Spectroscopy. FTIR analysis characterized the organic matter in the lampblack carbon. Samples were prepared by grinding the lampblack and mixing it with KBr and by forming the mixture into a pellet using a hand press. Transmission FTIR analysis was performed on a Nicolet 760 FTIR instrument. The use of this instrument for the characterization of organic matter in dredged sediment particles has been described by Ghosh et al. (*14*). CPMAS ^{13}C

solid-state NMR was conducted on the CA-10 soil as well as the separated lampblack fraction in order to determine the percentage of aliphatic and aromatic carbons present in the lampblack residuals. ^{13}C NMR spectra were obtained using a Varian VXR/Unity 400 MHz spectrometer with a wide-bore 9.4 T magnet at a ^{1}H frequency of 400 MHz and a ^{13}C frequency of 100.6 MHz. Lampblack samples were packed into in a 4 mm diameter Si_3N_4 rotor and spun at 14.1 kHz in a Doty Scientific MAS probe at the magic angle (54.7° to the magnetic field). NMR spectra were acquired with standard cross polarization (CP) and Bloch decay (no CP) pulse sequences. For both types of spectra, 1-s recycle delay time was used, and no changes in peak shapes were observed for longer pulse delays.

Total Extractable Organics (Oil and Grease). Three successive ultrasonic extractions with a 50:50 mixture of hexane and acetone were used to separate the oil phase in the lampblack sample as outlined in the PAH analysis. The mass of total extractable organics (TEO) was determined gravimetrically by evaporating the solvent from 25 mL of the hexane/acetone extract at room temperature. The percentage total extractable organics in lampblack was calculated by dividing the measured mass of total extractable organics by the mass of the solid sample. This method is similar to SW-846 EPA Method 9071A for oil and grease measurement in soil, sediments, and other solid materials. The difference is use of an ultrasonic extraction procedure instead of a Soxhlet extraction and a 50:50 hexane/acetone mixture instead of pure hexane as in the standard method. It was determined from comparative tests that TEO values obtained by ultrasonic extraction are very close to those by Soxhlet extraction, with differences smaller than 5%. Oil and grease is an operationally defined parameter, and the results depend on the extracting solvent and extraction method. Thus, TEO values measured in our study represent a convenient assay for oil and grease.

Batch Aqueous Equilibrium Tests. Complete phase separation in the lampblack−water systems is difficult to achieve by traditional filtration or centrifugation techniques owing to the small particle size and low density of lampblack. Two aqueous equilibrium measurement techniques were used to address colloids separation issues.

(i) An **air-bridge system** configuration was similar to that described by Bucheli and Gustafsson (*15*). In this setup, a 150-mL glass beaker containing about 5 g of lampblack sample, 120 mL of deionized (DI) water, and a stir bar was placed in a 4-L glass jar with Teflon-lined cap, and the annular space between the jar and the beaker was filled with 800 mL DI water. The 500 mg/L sodium azide (NaN_3) was added to the aqueous phase in the beaker and the annular space outside the beaker to prevent PAH degradation caused by incidental bacteria growth. The glass jar was then sealed with Teflon tape and equilibrated for 1−3 months on a magnetic stirrer to gently mix the solid slurry and facilitate solute transfer. In this setup, the beaker contains the solid slurry, and the annular compartment outside the beaker contains the aqueous phase. The exchange of PAH solutes between the two reservoirs and eventual equilibration takes place via the remaining air volume thus avoiding direct solids contact with the aqueous compartment. The aqueous phase sampled from the outer compartment was extracted by hexane three times. Then the extracts were analyzed by GC for PAHs. Bucheli and Gustaffson (*15*) found that aqueous equilibrium was reached in a 25 °C test within 14 d for phenanthrene and 14−31 d for pyrene. Previously, Kujawinski et al. (*16*) studied the PCB binding affinity of dissolved organic carbon (DOC) in protozoan and bacterial culture filtrates (<0.2 μm) using a similar experimental system comprising two nested beakers with a common headspace. They showed that the concentrations of spiked PCB congener in the inner beaker and outer beaker reached steady values after approximately 40−48 h.

(ii) An **alum flocculation method** developed by Ghosh et al. (*17*) involved a combination of centrifugation and alum flocculation of colloidal particles. In this method, the lampblack−water equilibrium tests were conducted in 1-L amber glass bottles with Teflon-lined caps with site material and water in the weight ratio of 1:20 and gently agitated on a horizontal shaker for 1 week to allow complete mixing and full contact between solid and water. Prior to the experiments, 500 mg/L sodium azide (NaN_3) was added to the system to inhibit bacteria growth. To ensure aqueous equilibrium and phase separation within the lampblack−water system, these bottles were then equilibrated for 5 months before sampling. After the contact period and settling, some of the lighter lampblack fraction of the sample floated to the surface with the heavier sand/clay fraction settling to the bottom. A clear aqueous phase formed between those two layers, and this clear layer was sampled using a 100-mL glass pipet to avoid disturbing the topmost layer of the lampblack fraction. The first 100 mL of sampled solution was used to condition the pipet, and the centrifuge tube and was discarded. The next 120 mL solution pipetted was collected in 150-mL glass centrifuge tubes. Replicate centrifuge tubes of aqueous phase samples were prepared from each bottle for PAH analysis. Shorter-term, 2-month contact tests were conducted with CA-10 and CA-17 samples, and comparison of the results of 5- and 2-month contacts gave similar aqueous PAH concentration values. Only the results from the 5-month aqueous equilibrium tests with alum flocculation method are reported in this paper due to the availability of a complete experimental data set for all soil samples in this study.

To remove colloidal particles from solution without sacrificing aqueous PAH composition integrity, the centrifuge tube contents were centrifuged at 4000*g* for 10 min to settle any coarse particles. This step was followed by the addition of 1.5 mL of 0.1 M alum solution and adjustment of pH back to neutral with 1 N NaOH solution. The supernatant water was mixed carefully using a glass pipet for 1 min to mix and flocculate the alum without disturbing the settled particles. Sweep floc was formed in less than 1 min, which was subjected to centrifugation for 30 min at 2000*g*. The clear supernatant was pipetted into a separatory funnel containing 10 mL of hexane as extraction solvent. About 5 mL of hexane was used to rinse the pipet, and the hexane was combined with the sample. The aqueous sample was extracted 3 times using fresh volumes of hexane with vigorous shaking for 3 min each. The final extract was dried with anhydrous sodium sulfate and concentrated to 0.2−1 mL for analysis.

Results and Discussion

Examination of five lampblack soil samples under a light microscope revealed the presence of sands, clays, and lampblack aggregates. The lampblack particles were identified by their black, sooty, and amorphous nature. The sand and clay particles appear more crystalline and are typically white and brown in color, respectively. Scanning electron microscopy, infrared spectroscopy, and solid-state NMR confirmed these visual observations. Scanning electron microscopy images of Fisher lampblack particles and one of the field lampblack samples CA-2 are shown in Figure 1. Lampblack appears as agglomerates of condensed solid spherical particles, as revealed in other microscopic investigations of oil soot (*10*). The individual particle size of Fisher lampblack is different from the field lampblack samples in this study. The Fisher lampblack particles were largely in the range of tens and hundreds of nanometers in size (Figure 1a). CA-2 as well as the other field lampblack samples (not shown) have much larger particle sizes ranging from submicron to about 1 μm (Figure 1b). Others report individual

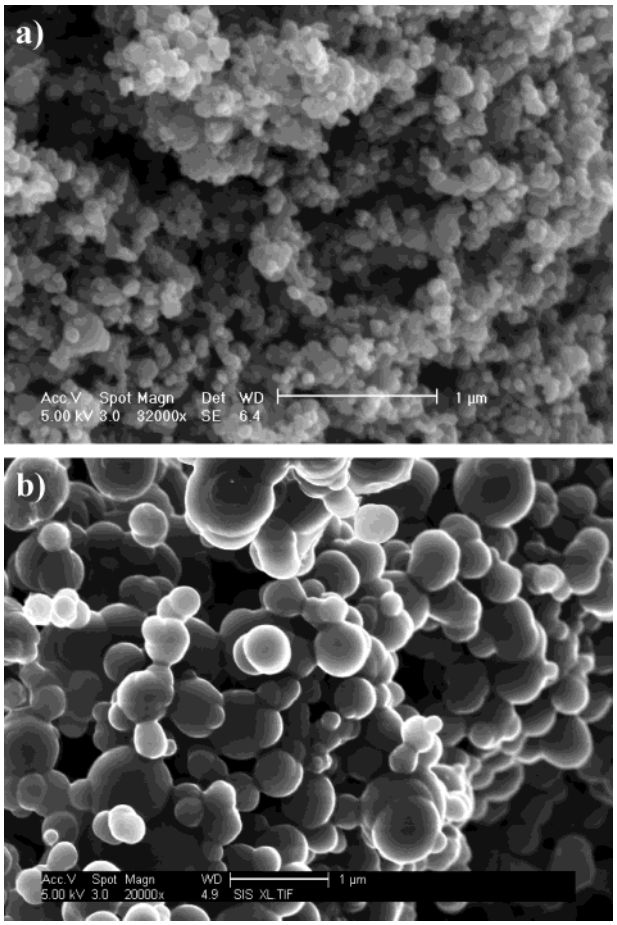

FIGURE 1. Scanning electron microscopy images of Fisher lampblack (a) and extracted CA-2 (b) showing a condensed, globular material with soot-like structure. The individual particle sizes of Fisher lampblack are in the range of tens to hundreds of nanometers, while CA-2 has larger individual particle sizes ranging from submicron up to about 1 μm.

lampblack particle diameters of 65 nm (*18*) and 80−100 nm for hexane soot (*19*). The specific surface area of raw lampblack field samples ranged from 1.3 to 4.9 m^2/g. The specific surface area of the Fisher lampblack was 29 m^2/g, consistent with a typical value of 22 m^2/g (*18*). As reported later, we found that the field lampblack samples contained various amounts of extractable oils. CA-10 had the highest oil content (9.1%) and correspondingly the lowest surface area (1.3 m^2/g). Thus, we surmised that oil was filling the interior pores, giving a low surface area measurement. Reanalysis of the surface area of CA-10 lampblack after extraction of oil by the TEO procedure gave 26 m^2/g and confirmed that the interior pores of CA-10 sample contained appreciable oily matter.

The elemental nature of the lampblack and sand/clay particles was determined by electron microscopy with EDS analysis. The lampblack particles are composed primarily (>95%) of carbon and contain only very small amounts of oxygen and sulfur. Sulfur is a common impurity in lampblack (*20*), and oxygen is likely to originate from water that may be adsorbed to the surface. Our results are consistent with the published literature, which reports that commercial lampblack is essentially 99.5% elemental carbon with much smaller amounts of oxygen and hydrogen (*21*). Oil-furnace carbon blacks used in the rubber industry contain 97−99% carbon with small amounts of hydrogen, oxygen, and sulfur (*18*). The sand/clay particles show high contents of silicon and oxygen, indicating the presence of large quantities of silica.

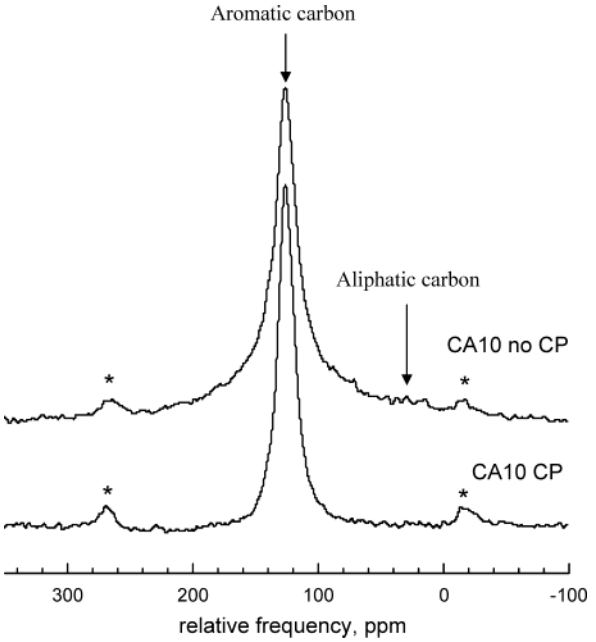

FIGURE 2. CPMAS ^{13}C solid-state nuclear magnetic resonance (NMR) spectra of CA-10 lampblack sample showing the predominantly aromatic nature of the carbon.

The organic character of lampblack residuals was investigated using FTIR and NMR analyses. The most prominent feature of the FTIR spectrum of lampblack is very little, if any, aliphatic C−H stretching around 2800 cm^{-1}. Aromatic C−H stretching around 3030 cm^{-1} is also barely present. The prominent peaks are at 1000 cm^{-1} and between 3200 and 3600 cm^{-1}. These peaks are likely to be from silica and the OH group of water that may have sorbed onto the lampblack, respectively. A less distinct peak appears around 1600 cm^{-1}, probably arising from C═C aromatic stretching. These FTIR observations agree with those presented by Akhter et al. (*19*) for hexane soot. The ^{13}C NMR spectra of the raw CA-10 sample with standard CP and Bloch decay (no CP) pulse sequences are depicted in Figure 2. In both spectra, a very prominent peak occurs between 100 and 150 ppm, indicating that almost all the carbon in the sample is aromatic. There are no real peaks in the region between 10 and 50 ppm, which implies negligible amounts of aliphatic carbon in the mixture. The peaks marked by asterisks on either side of the main peak are from the spinning sidebands. ^{13}C NMR spectroscopy studies of the separated lampblack fraction of CA-10 yielded the same results. The ^{13}C NMR spectrum for hexane soot is similar to that for the lampblack residuals with a prominent peak at 120−130 ppm coming from aromatic species with spinning sidebands at 230 and 25 ppm (*19*).

***μL^2*MS Analysis of PAHs in Lampblack Residuals.** Figure 3 presents the μL^2MS spectra of PAH distributions in the five raw soils. The instrument reports PAHs on sample surfaces desorbed from an area encompassed by a 40-μm laser shot; the spectra shown here are 50-shot averages at various locations on a lampblack sample. The results of all five samples show the same characteristic PAH patterns in all the residuals, although the relative abundance differs. On the basis of parent mass, the identified PAHs are naphthalene (128 Da), phenanthrene/anthracene (178 Da), pyrene/fluoranthene (202 Da), chrysene/benz[*a*]anthracene (228 Da), benzo[*b*]fluoranthene/benzo[*k*]fluoranthene/benzo[*a*]pyrene (252 Da), benzo[*g*,*h*,*i*]perylene/indeno[1,2,3-*c*,*d*]pyrene (276 Da), and dibenzo[*b*,*d*,*e*,*f*]chrysene (302 Da). In all the spectra, smaller PAH peaks appear at 326, 350, 374, and 398 Da and the series continues up to 600 Da. These higher molecular weight peaks differ by 24 Da, which results from

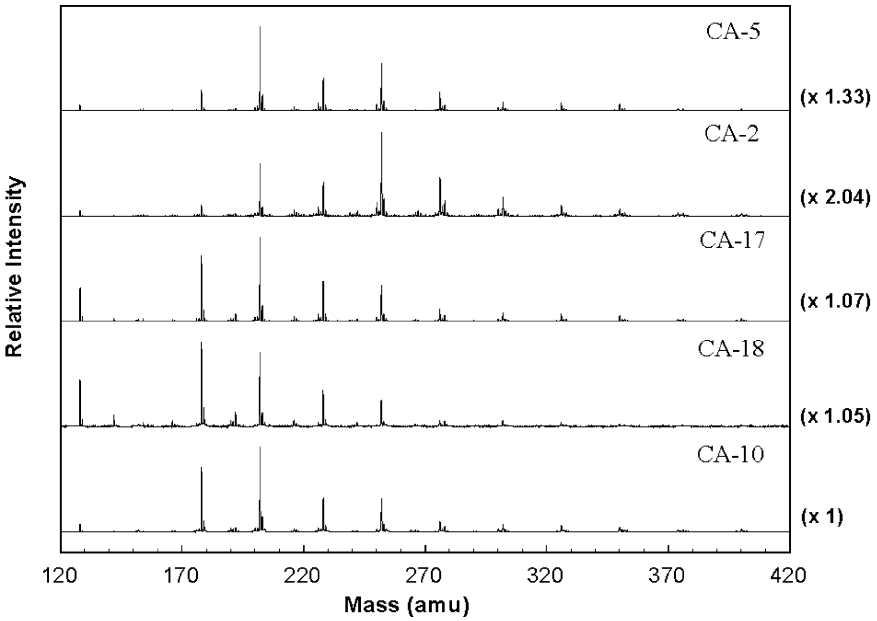

FIGURE 3. Microprobe laser desorption laser ionization mass spectra (μL^{2}MS) of PAHs in lampblack showing the unique distribution of PAHs in lampblack samples with a succession of parent PAH compounds lacking alkyl substituents.

the consecutive completion of an additional benzene ring to the already existing PAH compound with four of the carbon atoms of the new ring being shared among existing rings. This PAH distribution is rather unusual in that the PAH pattern lacks alkyl substituents and is unlike μL^{2}MS spectra observed for PAHs in contaminated soils from coal gas manufacture (*13*) or dredged harbor sediments (*14*). A comparison of the peak areas corresponding to the parent and alkylated PAHs shows that parent PAHs in the lampblack samples comprised over 95% of the total PAHs. Lampblack in the Pacific Coast oil−gas process was formed at 1600 °F and higher temperatures (*1*). At these temperatures, less stable alkyl bonds of PAH compounds are rapidly cleaved (*22*), and a PAH distribution lacking an alkylation pattern is expected. The μL^{2}MS and GC-FID results indicate that the levels of alkylated PAHs in the lampblack samples are very low, consistent with the fact that the PAHs are being formed at high temperature, typically between 1200 and 1800 °F.

Fisher lampblack and weathered coal tar from a carbureted water gas site were analyzed by μL^{2}MS to determine how the PAH distributions of the lampblack residuals compare with that of standard lampblack material and aged coal tar. Figure 4 compares these spectra with a lampblack residual. The commercial lampblack has a distinct and simple PAH distribution in that only two prominent PAH peaks are evident, pyrene/fluoranthene (202 Da) and lower relative amounts of phenanthrene/anthracene (178 Da). There are much smaller peaks at 228, 252, and 276 Da and negligible amounts of alkylated PAHs as would be expected based on the high temperature formation of lampblack. The PAH distribution for the weathered coal tar shows predominant peaks at 178 and 202 Da, associated methyl substituents that are displaced by 14 Da with peaks at 192 and 216 Da, and smaller peaks to about 276 Da. In summary, each sample has a distinct PAH fingerprint.

Bulk Analysis of Lampblack-Impacted Soils. Table 1 shows the total concentration of 16 EPA priority pollutant PAHs in the five lampblack-impacted site samples. The PAH concentrations vary greatly depending on the site. CA-10 was the most contaminated site sample with 35 200 mg/kg, 25 times as much as CA-5, the least contaminated site sample with 1410 mg/kg PAHs. The site samples also vary in PAH distribution patterns. CA-5 and CA-10, despite having a factor of 25 difference in total PAHs, have a similar distribution comprising mainly PAH compounds of moderate and high molecular weight with pyrene, benzo[*g*,*h*,*i*]perylene, and fluoranthene accounting for half of the total PAHs. The distribution of PAH compounds in CA-17 and CA-18 show that lower molecular weight PAH compounds are more abundant. Naphthalene and phenanthrene comprise 23% of the total PAHs for CA-17 and 39% for CA-18. A common characteristic of the PAH distribution patterns for the five lampblack field samples is that fluoranthene and pyrene are major PAH compounds existing in the lampblack-impacted soil samples. Oil−gas plants ceased operation 60−90 years ago, and contemporaneous lampblack samples are not available, and site-specific residuals management practices are not known. Thus, it is difficult to assess whether the ratio of lower molecular weight PAHs versus higher molecular weight PAHs reflects differences in disposal and burial and weathering or differences in process conditions. Weathering indexes that are used to assess the degradation of crude oils over time are of limited use with these samples.

For Fisher lampblack, the total PAH concentration is 700 mg/kg, and fluoranthene and pyrene are the predominant PAH compounds with a combined contribution of about 76% of the total PAH concentration present in the commercial lampblack. The PAH distribution pattern in the commercial lampblack is consistent with results of bulk analysis for five lampblack-impacted site samples in that fluoranthene and pyrene are the dominant PAH compounds in the field samples.

The percentage of total extractable organics was used to estimate the level of oily matter present in the raw lampblack samples. Results presented in Table 1 show lampblack-impacted soil samples have high levels of extractable oily matter (by weight) ranging from 1.5% for the CA-5 sample to 9.1% for the CA-10 sample. As noted in the Introduction, the oil or tar content of lampblack varies with process and separation scheme, and whether tar was added to lampblack for briquetting or for boiler fuel. Morgan (*1*) notes that lampblack may contain from 6 to 14% tar by extraction. The Fisher lampblack characterized in this study has fairly low oil content of 0.1 wt % as compared with a typical oil content of around 1 wt % in commercial lampblack (*12*).

PAHs in Separated Fractions. The raw lampblack samples were separated by density into a lighter density lampblack fraction and a heavier density sand/silt/clay fraction with

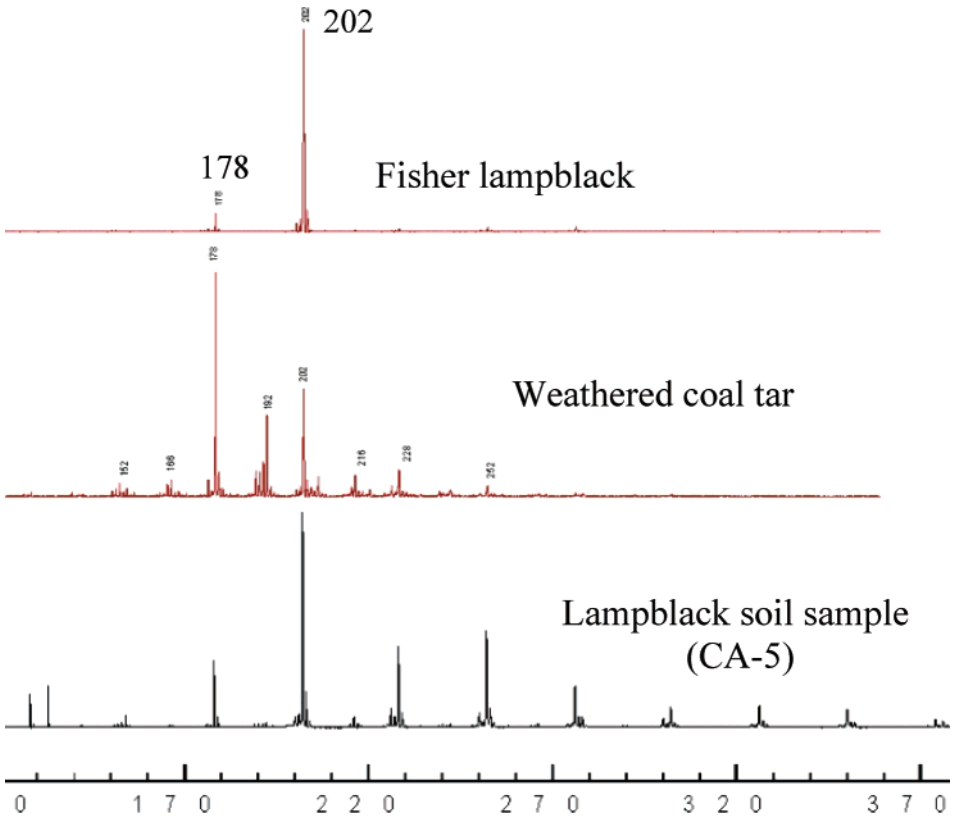

FIGURE 4. Comparison of μL^{2}MS PAH mass spectra of Fisher lampblack sample, a weathered coal tar sample from a manufactured gas plant site, and a lampblack soil sample. The Fisher lampblack contains two major PAH mass peaks (178 and 202). The weathered coal tar sample shows both parent PAHs and methylated PAHs, whereas the lampblack soil sample shows only the parent PAHs. Each sample has a characteristic PAH fingerprint.

TABLE 1. Sum of 16 EPA Priority Pollutant PAHs, Extractable Oily Matter (Oil and Grease), and Total Organic Carbon (TOC) Content of Study Lampblack-Impacted Soils and Fisher Lampblack

	total PAHs (mg/kg)[a]	oily matter (wt %)	TOC (wt %)	lampblack fraction (wt %)	% of total PAHs on lampblack fraction
Fisher LB	700	0.1		100	100
CA-5	1 410	1.5	14	22	96
CA-2	8 350	4.9	71	65	100
CA-17	12 700	3.9	47[b]	53	95
CA-18	17 600	4.9	50	62	81
CA-10	35 200	9.1	94	84	99

[a] mg/kg soil for the five field soil samples and mg/kg lampblack for the Fisher lampblack. [b] Reported by Steven B. Hawthorne, University of North Dakota.

PAH analyses performed on both of the separated components. The mass percentage of lampblack in the samples ranged from 22% for CA-5 to 84% for CA-10, as shown in Table 1. Also shown in Table 1 are the percentages of the total PAHs present on the lampblack fraction in the five samples. The majority of the PAHs (81−100%) are associated with the lighter density lampblack fractions. There was no significant difference between the PAH distribution pattern for lampblack or sand/clay, which suggests the possibility that entrained lampblack particles might be present in the heavier mineral fraction and were not completely removed by density separation.

Control Studies with Pure PAHs To Test Equilibration Methods. In control experiments of the air-bridge system using solid PAHs, equilibration between the two reservoirs was reached within 10−20 d for phenanthrene and nearly 60 d for pyrene at the lab temperature of 16.5 °C. These results

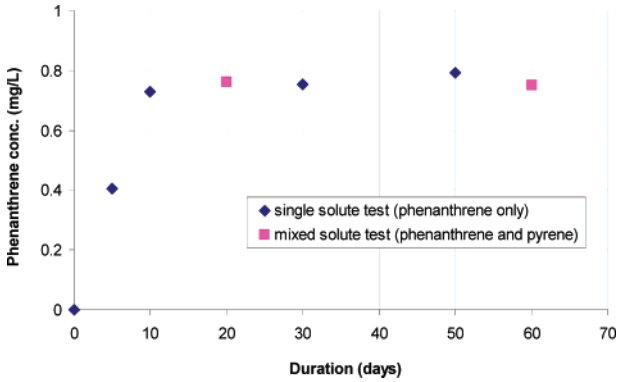

FIGURE 5. Change in aqueous phenanthrene concentration with time in control tests with pure phenanthrene and a phenanthrene/pyrene mixture using an air-bridge equilibrium system.

agree with Bucheli and Gustaffson's (*15*) finding that at 7 °C equilibration was reached within 10−33 d for phenanthrene and 33−80 d for pyrene and that at 25 °C equlibration was reached within 14 d for phenanthrene and 14−31 d for pyrene. Figure 5 presents the change of aqueous concentration of phenanthrene over time in both single solute and mixed solutes control tests. In the control test with only pure phenanthrene crystals, the aqueous concentration reached 0.73 mg/L within 10 d, increasing to 0.75 mg/L after 30 d and staying at this level. In the control test with both phenenthrene and pyrene as solutes, after 20 d the aqueous concentration of phenanthrene was 0.76 mg/L, essentially the same as the measurement of 0.75 mg/L after 60 d. The measured solubility agreed well with a calculated aqueous solubility of solid phenanthrene at 16.5 °C, which ranges from 0.65 to 0.80 mg/L depending on estimation method (*23*−*25*). The equilibration behavior of pyrene in the air-

TABLE 2. Effect of Alum Flocculation on Aqueous PAH Concentration Measurement[a]

compd	control test (μg)	mass in aq phase after floc (μg)	mass on glass and floc (μg)	loss on glass and floc (%)
phenanthrene	3.941 ± 0.011	3.891 ± 0.059	0.022 ± 0.001	0.56 ± 0.03
pyrene	4.633 ± 0.012	4.486 ± 0.004	0.106 ± 0.022	2.28 ± 0.47

[a] Data shown are average values of duplicate tests.

bridge system was investigated in the mixed solutes control test; the aqueous concentration was 0.069 mg/L when sampling at 20 d and 0.075 mg/L at 60 d. This latter value is close to the calculated solubility of solid pyrene at 16.5 °C, which ranges from 0.083 to 0.097 depending on estimation method (*23*−*25*).

A possible concern with the use of alum flocculation for colloid removal was sorption of PAHs on the alum floc during particle separation. Control tests were conducted to assess whether PAHs would sorb on the alum floc and affect the measurement of aqueous phase PAH concentrations. Test PAH solutions containing phenanthrene and pyrene were used for this purpose. A 10-μL sample of the stock PAH solution (approximately 0.6 g/L in acetone for both phenanthrene and pyrene) was spiked in 150-mL centrifuge tubes filled with 120 mL of DI water and agitated on a horizontal shaker for 2 h before alum flocculation. Three consecutive liquid−liquid extractions using hexane were performed on the supernatant with GC analysis of PAHs in the extract. To make a mass balance analysis, after draining the supernatant, the centrifuge tube was rinsed 3 times with hexane to collect any PAHs possibly left in the flocculent and/or glass. The extracts were then combined, dried, and analyzed by GC. Control tests were also conducted to determine the exact mass of phenanthrene and pyrene added to the sample solution. Results of PAH concentrations recovered from tests using alum treatment and the control tests are shown in Table 2. Only 0.6% of phenanthrene and 2.3% of pyrene were lost during the alum flocculation process, and thus the effect of the alum flocculation procedure on aqueous-phase PAHs was considered negligible.

Aqueous Equilibrium Measurements of Lampblack Samples. Aqueous equilibrium experiments were conducted with the lampblack samples using both the air-bridge method and the alum flocculation method. Figure 6 compares the results using these two equilibration techniques for two of the samples. The aqueous concentration measurements agree well between the two methods. The advantage of the air-bridge method is the ease of sampling large volumes of water needed for the detection of low-level aqueous PAH concentrations. The results of aqueous equilibrium using the air bridge measurements of the six lampblack samples are shown in Figure 7. For three of the samples (CA-10, CA-17, and CA-18), aqueous equilibrium concentrations are in the tens and hundreds of micrograms per liter, nearly 2−3 orders of magnitude greater than those for the remaining three (CA-2, CA-5, and Fisher lampblack). As calculated from total PAH concentrations and TOC contents of soil samples shown in Table 1, the organic carbon normalized total PAH concentrations for CA-10, CA-17, and CA-18 are a factor of 3 higher than for CA-2 and CA-5, thus the 2−3 orders of magnitude difference in aqueous equilibrium concentrations is not explained by the 3 times higher organic carbon-normalized PAH concentrations in the first set of three samples.

Prediction of Aqueous Equilibrium Partitioning from Lampblack Samples. To understand the aqueous partitioning behavior of PAHs in lampblack-impacted soils, two modeling approaches were evaluated. In the first model, all PAHs in the lampblack soils were assumed to be associated with the lampblack carbon, and measured partition coefficients for oil−soot from Jonker and Koelmans (*10*) were

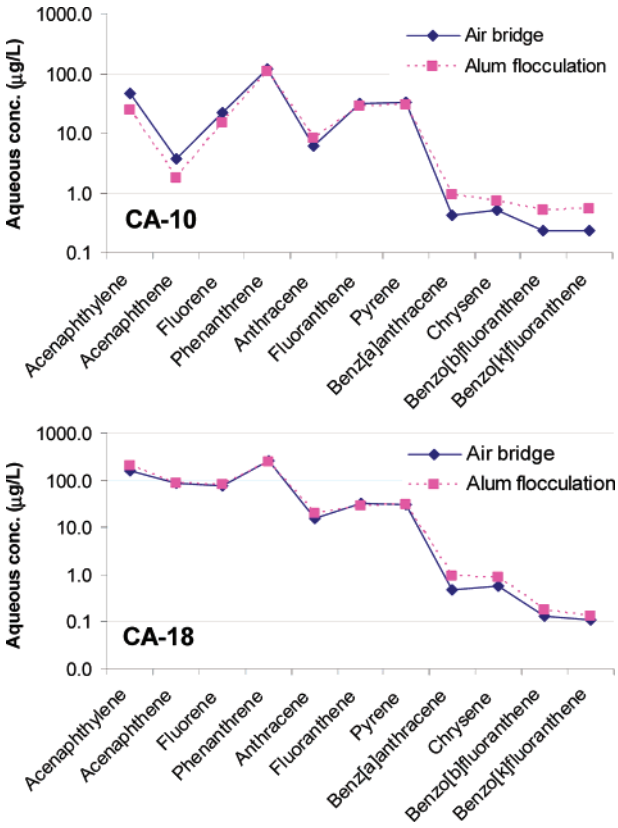

FIGURE 6. Comparison of aqueous equilibrium concentrations measured with the air-bridge and alum flocculation techniques. Results from these two measurement techniques agree closely.

used to describe the partitioning, as shown in

$$C_i^{aq} = \frac{C_i^{solid}}{f_{oc}K_{oc}} \quad (1)$$

where C_i^{aq} is the aqueous-phase concentraion of PAH i (mg/L), C_i^{solid} is the solid-phase concentration of PAH i (mg/kg), f_{oc} is the fraction organic carbon of lampblack soil (Table 1), and K_{oc} is taken from Jonker and Koelmans (*10*) data for oil soot and for native PAH compounds. Since the K_{oc} values for acenaphthylene, acenaphthene, and fluorene were not reported in their study for oil soot, we applied the oil−soot partitioning model to phenanthrene, anthracene, fluoranthene, and pyrene with the available data.

The second model assumed that all PAHs were present as an oil phase and that the partitioning was between water and the aromatic oil phase. The approach of Peters et al. (*26*) for coal tar was used to model PAH partitioning from the oil phase. In this approach, the aqueous concentration of a PAH is calculated using eq 2, where x_i is the mole fraction of PAH i and S_i is the subcooled liquid solubility of PAH i. The subcooled liquid solubility is calculated using eq 3, where C_i^* is the aqueous solubility of the solid PAH i and $(f^s/f^l)_i$ is the ratio of solid−liquid reference fugacities for the pure PAH i. Pure compound aqueous solubilities and fugacity ratios are

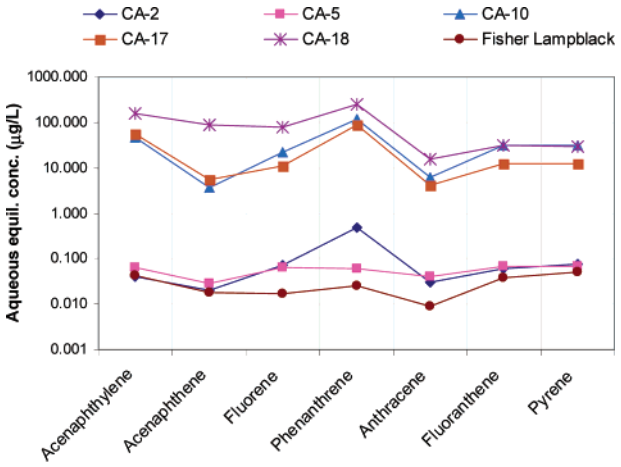

FIGURE 7. Aqueous equilibrium concentrations of PAHs for the six study materials as measured by the air-bridge technique. CA-2, CA-5, and Fisher lampblack show nearly 2−3 orders of magnitude lower PAH concentrations in the aqueous phase as compared to the other lampblack-impacted soils including CA-10, CA-17, and CA-18.

from the data summarized by Peters et al. (*26*).

$$C_i^{aq} = x_i S_i \tag{2}$$

$$S_i = \frac{C_i^*}{(f^s/f^l)_i} \tag{3}$$

The soot partitioning and oil partitioning models were evaluated for the six lampblack samples, and the aqueous concentration predictions were compared with the measured values. Modeling results for one representative lampblack sample showing high aqueous equilibrium PAH concentrations (CA-10, in Figure 8a) and one lampblack sample showing low aqueous equilibrium PAH concentrations (CA-2, in Figure 8b) are discussed in this paper. Data in Figure 8a,b are reported as apparent partition coefficients, K_d (PAH concentration in solid phase/PAH concentration in aqueous phase) to account for the differences in PAH levels. The aqueous partitioning of the seven PAHs predicted based on the two modeling approaches differ by 1.5−2 orders of magnitude. A much smaller K_d is predicted with the oil−water partitioning model as compared to the soot−water partitioning model. For lampblack soil sample CA-10 (and also CA-17 and CA-18, data not shown), the measured partitioning values compare well with the oil−water partitioning model, whereas for lampblack soil sample CA-2 (and also CA-5 and Fisher LB, data not shown), the measured partitioning values compare well with the soot partitioning model. Thus, for three of the lampblack samples that have relatively low levels of PAHs, partitioning into water is similar to that of soot−water partitioning, and for the three samples that have high PAH levels (>12 000 mg/kg), PAH partitioning appears to mimic that of oil−water partitioning. A possible explanation for these observations is that at high levels of PAHs, the soot surfaces may be completely covered leading to the creation of a free PAH−oil phase coating. The strong binding of PAHs to the soot−carbon matrix is attributed to the overlap of π-electrons in the aromatic soot structure and the planar aromatic rings of PAH molecules. PAHs in the excess oil phase do not experience binding with the aromatic soot surface and behave more like a free oil phase as shown schematically in Figure 9. This explanation assumes a Langmuir-like mechanism (i.e., monolayer sorption to the available soot surface) with excess PAHs not binding to the solid substrate.

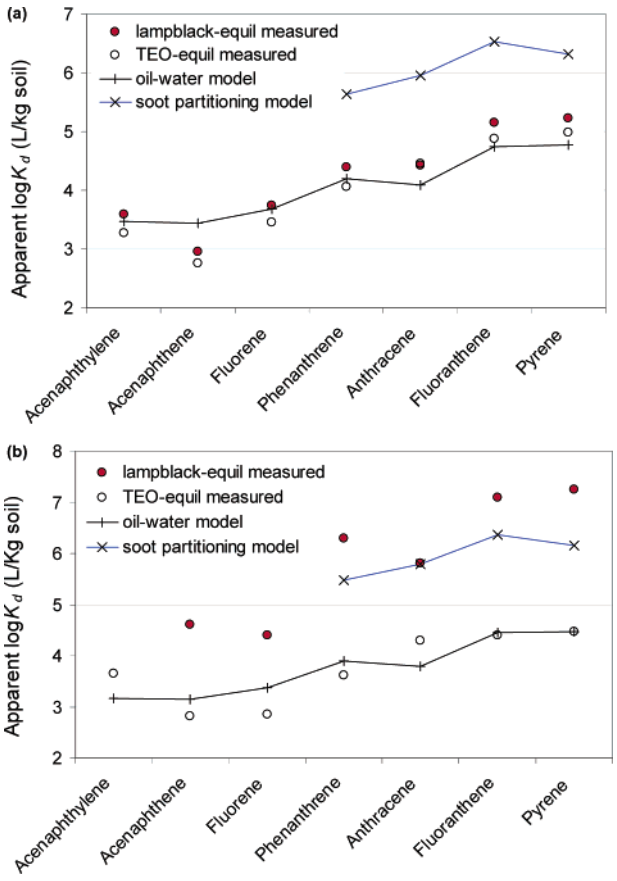

FIGURE 8. (a) Apparent PAH partition coefficients (K_d) for CA-10 lampblack-impacted soil show good agreement with predictions based on the aromatic oil−water partitioning model. In comparison, predictions based on the soot-partitioning model are more than an order of magnitude higher than the measured values. K_d values based on aqueous equilibrium measurements of the extracted oil alone agree very well with the lampblack−soil and the oil−water partitioning model. Apparent K_d values for the oil equilibrium are expressed as the ratio of PAH whole soil sample concentration to the PAH aqueous concentration. (b) Apparent PAH partition coefficients (K_d) for CA-2 lampblack-impacted soil show good agreement with predictions based on the soot partitioning model. In comparison, predictions based on an oil−water partitioning model are more than 1 order of magnitude smaller. K_d values based on aqueous equilibrium measurements of the extracted oil alone agree with the oil−water partitioning model and are much smaller as compared to those observed for the whole lampblack soil. Apparent K_d values for the oil equilibrium are expressed as the ratio of PAH whole soil sample concentration to the PAH aqueous concentration.

Results from Extracted Oil Equilibrium Tests. To investigate further the effect of oil in the lampblack soil samples on aqueous-phase partitioning, aqueous equilibrium tests were conducted with the extractable oils of CA-10 and CA-2 using the air-bridge method. The results of aqueous equilibrium measurements are shown in Figure 8a,b as apparent partitioning coefficients K_d. For ease of comparison, partition coefficients for both lampblack soil equilibrium and oil equilibrium are expressed as PAH concentration in the whole solid sample divided by aqueous PAH concentration. Thus, the aqueous equilibrium measurements are normalized to the original solid-phase concentration to remove the effect of varying levels of the different PAHs. For CA-10, both whole lampblack-impacted soil and extracted oil provide similar aqueous concentrations at equilibrium, which are predicted based on an oil−water partitioning model. This behavior implies that the sorption capacity of the lampblack carbon

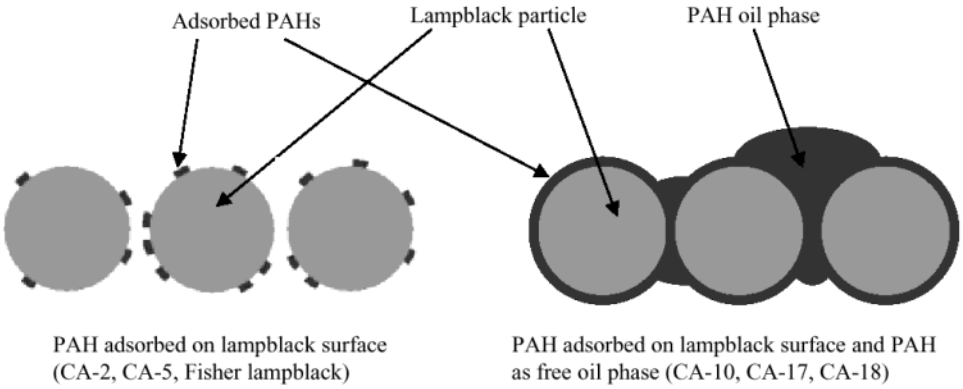

FIGURE 9. Schematic of lampblack particles with PAHs adsorbed on available surface at low PAH concentrations (as in field samples CA-2, CA-5, and Fisher lampblack) shown on the left. When PAHs are in excess of available sorption sites, a free PAH oil phase may form as illustrated on the right (as in field samples CA-10, CA-17, and CA-18).

in CA-10 is exhausted and that the excess PAH mixture forms a free oil phase that controls PAH partitioning. To test if the reverse would be true for a soil that has low PAH levels, extracted PAH oil phase from CA-2 soil sample also was evaluated in aqueous equilibrium experiments. Unlike CA-10, PAH aqueous equilibrium measurements for CA-2 oil extract were 1−2 orders of magnitude higher than for the whole soil. Thus, for lower PAH concentrations in the presence of available lampblack carbon sorption sites, PAH partitioning is similar to soot−water partitioning. However, on extracting the PAHs, removing the lampblack carbon and allowing the PAH mixture to form a PAH oil phase in the absence of aromatic carbon sorption sites, equilibrium partitioning behavior appears close to that of oil−water partitioning. This observation provides stronger evidence to the explanation that for lampblack samples CA-10, CA-17, and CA-18 with high PAH levels, a free oily phase plays a dominant role in the PAH aqueous partitioning, whereas for lampblack samples CA-2, CA-5, and Fisher lampblack with relatively lower PAH levels, the soot−carbon phase dominates the PAH aqueous partitioning.

This research illustrates the complexity involved in understanding the mechanisms controlling the binding of PAHs in field materials. Although much work has been done in the past on describing the binding of PAHs on pure black carbon materials (*7*−*10*), little work has been done in characterizing the nature of sorption and binding of native PAHs in field materials such as soils impacted from oil−gas manufacturing facilities. Because of the predominance of soot-type carbon in lampblack and the known high PAH sorption capacity of soot−carbon, one might expect diminished aqueous leaching and impact from lampblack soils. This behavior was found to be true for two of the field samples studied (CA-2 and CA-5), but for three field samples of lampblack soils (CA-10, CA-17, and CA-18), a high leaching potential of PAHs was observed similar to what may be expected from coal tar. In these high leaching lampblack soil samples, the PAH sorption capacity of the soot appears exhausted, and the presence of a free-phase aromatic oil tar is suspected. Thus, for field samples from oil−gas manufacturing sites, the relative amounts of soot and PAHs determine whether there is a diminished water leaching as for soot−carbon or a relatively high leaching as for a PAH−oil. For low PAH loadings per gram of soot−carbon, soot−water partitioning may be expected. For high PAH loadings per gram of soot−carbon, partitioning as in coal tar−water systems can be expected. Whether soot−carbon or PAH−oil is the governing phase for PAH partitioning results in as much as 2−3 orders of magnitude difference in aqueous equilibrium concentrations of PAHs.

We compared the aqueous equilibrium concentrations of PAHs measured with field samples CA-2 and CA-10 with the California Regional Water Quality Control Board, San Francisco Bay Region groundwater Risk-Based Screening Levels (RBSLs) for drinking water sources (*27*). We found for CA-2, a representative soil sample with comparatively lower PAH and oil levels, that aqueous equilibrium concentrations of most PAHs examined in this study are less than or equal to the groundwater RBSLs except for benzo[*k*]fluoranthene and benzo[*a*]pyrene, which slightly exceeded the screening levels by a factor of 1−2. In contrast, for CA-10, a representative soil sample with high PAH and oil levels, aqueous equilibrium concentrations for 13 regulated PAHs are significantly greater than the groundwater RBSLs. This indicates that additional investigation and evaluation of potential risk may be warranted at sites where PAH and oil concentrations are high in lampblack-impacted soil and the leaching potential for PAHs from the site soil may be greatest, as for CA-10, CA-17, and CA-18. However for sites CA-2 and CA-5, even though the PAH contamination in the impacted soil is large, the low leaching potential of PAHs from the lampblack suggests that migration to the groundwater is not an important potential exposure pathway.

Generalized assessments based on soil organic carbon partition coefficients may lead to miscalculation of the risk from the leaching of PAHs from lampblack residuals. Recent work by Stroo et al. (*28*) demonstrated that site specific risk assessment for PAH contaminated oil−gas plant sites may result in environmentally protective cleanup levels that allow 3−10 times higher PAH levels than values derived from default risk assessment assumptions. To explain the reason for the differences in risk assessment, however, one needs to understand more fully the governing mechanisms that control PAH binding to the site materials. The present research provides a framework to assess PAH binding mechanisms that govern site-specific PAH leaching potential and availability assumptions for risk assessment of lampblack-impacted soils.

Acknowledgments

The Gas Technology Institute supported this work through a contract administered by The RETEC Group, Monroeville, PA. Elemental analyses were performed in the Department of Geology and Geophysics, University of California, Berkeley. ^{13}C solid-state NMR was conducted in the laboratory of Professor Jonathan Stebbins, Department of Geological and Environmental Sciences, Stanford University. Bob Jones in the Geballe Laboratory for Advanced Materials, Stanford University, assisted with SEM analyses.

Literature Cited

(1) Morgan, J. J. *A Textbook of American Gas Practice, Vol. 1, Production of Manufactured Gas*, 2nd ed.; Morgan: Maplewood, NJ, 1931.

(2) Luthy, R. G.; Dzombak, D. A.; Peters, C. A.; Roy S. B.; Ramaswami, A.; Nakles, D. V.; Nott, B. R. *Environ. Sci. Technol.* **1994**, *28*, 266A−276A.
(3) Harkins, S. M.; Truesdale, R. S.; Hill, R.; Hoffman, P.; Winters, S. *U.S. Production of Manufactured Gases: Assessment of Past Disposal Practices*; Research Triangle Institute, Hazardous Waste Engineering Research Laboratory, Office of Research and Development, U.S. EPA: Cincinnati, February 1988; EPA/600/2-88/012.
(4) U.S. EPA. *Sediment Quality Criteria for the Protection of Benthic Organisms: Phenanthrene*; U.S. Environmental Protection Agency, Office of Water: Washington, DC, 1993; EPA-882-R-93-014.
(5) Ghosh, U.; Zimmerman, J. R.; Luthy, R. G. *Environ. Sci. Technol.* **2003**, *37*, 2209−2217.
(6) Gustafsson, O.; Gschwend, P. M. In *Molecular Markers in Environmental Geochemistry*; Eganhouse, R. P., Ed.; ACS Symposium Series 671; American Chemical Society: Washington, DC, 1997; pp 365−381.
(7) Grathwohl, P. *Environ. Sci. Technol.* **1990**, *24*, 1687−1693.
(8) Accardi-Dey, A.; Gschwend, P. M. *Environ. Sci. Technol.* **2002**, *36*, 21−29.
(9) Karapanagioti, H. K.; Kleineidam, S.; Sabatini, D. A.; Grathwohl, P.; Ligouis, B. *Environ. Sci. Technol.* **2000**, *34*, 406−414.
(10) Jonker, M. T. O.; Koelmans, A. A. *Environ. Sci. Technol.* **2002**, *36*, 3725−3734.
(11) Nelson, D. W.; Sommers, L. E. Total Carbon, Organic Carbon and Organic Matter. In *Methods of Soil Analysis, Part 3. Chemical Methods;* Sparks, D. L., Ed.; Soil Science Society of America Book Series 5; American Society of Agronomy: Madison, WI, 1996; pp 961−1010.
(12) *Polynuclear Aromatic Compounds, Part 2, Carbon Blacks*, Vol. 33; IRAC Monographs on the Evaluation of the Carcinogenic Risk of Chemical to Humans; World Health Organization: Geneva, 1984.
(13) Gillette, J. S.; Luthy, R. G.; Clemett, S. J.; Zare, R. N. *Environ. Sci. Technol.* **1999**, *33*, 1185−1192.
(14) Ghosh, U.; Gillette, J. S.; Luthy, R. G.; Zare, R. N. *Environ. Sci. Technol.* **2000**, *34*, 1729−1736.
(15) Bucheli, T. D.; Gustafsson, O. *Environ. Sci. Technol.* **2000**, *34*, 5144−5151.
(16) Kujawinski, E. B.; Farrington, J. W.; Moffett, J. W. *Environ. Sci. Technol.* **2001**, *35*, 4060−4065.
(17) Ghosh, U.; Weber, A. S.; Jensen, J. N.; Smith, J. R. *Environ Sci. Technol.* **2000**, *34*, 2542−2548.
(18) Kroschwitz, J. I.; Howe-Grant, M. *Kirk-Othmer Encyclopedia of Chemical Technology*, 4th ed.; Wiley: New York, 1992; Vol. 4.
(19) Akhter, M. S.; Chughatai, A. R.; Smith, D. M. *Appl. Spectrosc.* **1985**, *39*, 143−153.
(20) Sokhi, R. S.; Gray, C.; Gardiner, K.; Earwaker, L. G. *Nucl. Instrum. Methods Phys. Res., Sect. B* **1999**, *B49* (1−4), 414−417.
(21) Kamegawa, K.; Nishikubo, K.; Yoshida, H. *Carbon* **1998**, *36*, 433−441.
(22) Mahajan, T. B. Ph.D. Dissertation, Stanford University, Stanford, CA, 2002.
(23) Wauchope, R. D.; Getzen, F. W. *J. Chem. Eng. Data* **1972**, *17*, 38−41.
(24) Getzen, F. W. In *Proceedings of the American Chemical Society Symposium on Ordered Fluids and Liquid Crystals*; Johnson, J. F., Porter, R. S., Ed.; Plenum: New York, 1970; p 53.
(25) May, W. E.; Wasik, S. P.; Miller, M. M.; Tewari, Y. B.; Brown-Thomas, J. M.; Goldberg, R. N. *J. Chem. Eng. Data* **1983**, *28*, 197−200.
(26) Peters, C. A.; Knights, C. D.; Brown, D. G. *Environ. Sci. Technol.* **1999**, *33*, 4499−4507.
(27) *Application of Risk-Based Screening Levels and Decision Making to Sites with Impacted Soil and Groundwater* (*Interim Final*−*December 2001*); California Regional Water Quality Control Board, San Francisco Bay Region: 2001; http://www.swrcb-.ca.gov/rwqcb2/rbsl.htm.
(28) Stroo, H. F.; Jensen, R.; Loehr, R. C.; Nakles, D. V.; Fairbrother, A.; Liban, C. B. *Environ. Sci. Technol.* **2000**, *34*, 3831−3836.

Received for review October 24, 2002. Revised manuscript received May 20, 2003. Accepted May 23, 2003.

ES0262683